Elements of X-RAY DIFFRACTION

SECOND EDITION

B. D. CULLITY
Department of Metallurgical Engineering and Materials Science
University of Notre Dame

ADDISON-WESLEY PUBLISHING COMPANY, INC.
Reading, Massachusetts · Menlo Park, California
London · Amsterdam · Don Mills, Ontario · Sydney

This book is in the
Addison-Wesley Series in Metallurgy and Materials

Morris Cohen
Consulting Editor

Second printing, October 1978

ISBN 0-201-01174-3
ABCDEFGHIJK-MA-798

counter, the counter slits must be as wide as the diffracted beam for all values of α so that the whole width of the beam can enter the counter. The ideal incident beam for this method is a parallel one. However, a divergent beam may be used without too much error, provided the divergence is not too great. There is no question of focusing here: if the incident beam is divergent, the diffracted beam will diverge also and very wide counter slits will be required to admit its entire width. Clockwise rotation of the specimen about the diffractometer axis makes the diffracted beam narrower and is therefore preferred to counterclockwise rotation.

The value of μt used in Eq. (9-10) must be obtained by direct measurement, since it is not sufficiently accurate to use a tabulated value of μ together with the measured thickness t of the specimen. To determine μt we use a strong diffracted beam from any convenient material and measure its intensity when the sheet specimen is inserted in the diffracted beam and again when it is not. The value of μt is then obtained from the absorption law, $I_t = I_0 e^{-\mu t}$, where I_0 and I_t are the intensities incident on and transmitted by the sheet specimen, respectively.

The *Schulz transmission method* [9.10] involves the use of a divergent, rather than a parallel, incident beam and a counter slit narrow enough to intercept only the central portion of the diffracted beam. For these conditions Schulz derived an equation, analogous to Eq. (9-9), relating the intensity diffracted by a random specimen (for brevity "random specimen" will be written for "specimen with randomly oriented grains") to the angular setting α. He also showed that the intensity diffracted by a random specimen was constant within a few percent up to an α value of about 30° for a sufficiently thin specimen ($\mu t = 0.4$ to 0.7) and small values of θ (less than about 20°); under these conditions the correction equation is not needed.

In tests of the correction equations by means of random specimens, Newkirk and Bruce [9.11] found good agreement with Eq. (9-10) of Decker, Asp, and Harker. On the other hand, the data of Aoki *et al.* [9.12] show better agreement between experiment and theory for the Schulz method than that of Decker *et al.* However, in judging the validity of correction equations one must always keep in mind the necessity not only of a truly random specimen, but also of a close match between the actual x-ray optics (nature of incident beam and width of counter slit) and those assumed in the derivation of the equations.

Reflection Methods

The central region of the pole figure is inaccessible to any transmission method and can be explored only by a reflection technique. The specimen must be of effectively infinite thickness or extra corrections will be required.

The most popular is the *Schulz reflection method* [9.13]. It requires a special specimen holder which allows rotation of the specimen in its own plane about an axis normal to its surface and about a horizontal axis; these axes are shown as BB' and AA' in Fig. 9-16. The horizontal axis AA' lies in the specimen surface and is initially adjusted, by rotation about the diffractometer axis, to make equal angles with the incident and diffracted beams. After this is done, no further rotation about the diffractometer axis is made. Since the axis AA' remains in a fixed position during the other rotations of the specimen, the irradiated surface of the specimen is always tangent to a focusing circle passing through the x-ray source and counter slit. A divergent beam may therefore be used since the diffracted beam will converge to a focus at the counter.

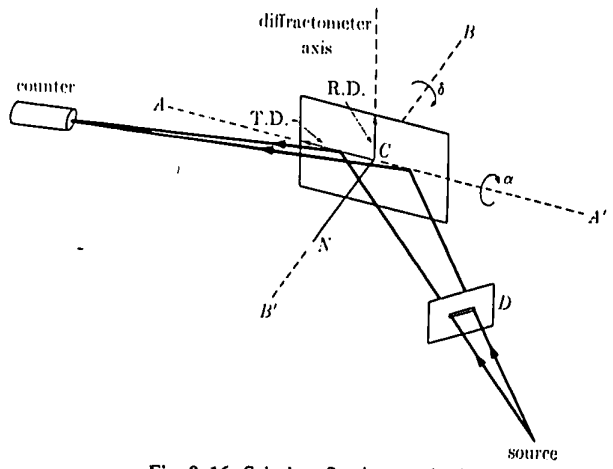

Fig. 9-16 Schulz reflection method.

When the specimen is rotated about the axis AA', the axis BB' normal to the specimen surface rotates in a vertical plane, but CN, the reflecting plane normal, remains fixed in a horizontal position normal to AA'. The rotation angles α and δ are shown in Fig. 9-16. The angle α is zero when the sheet is horizontal and has a value of 90° when the sheet is in the vertical position shown in the drawing. In this position of the specimen, the reflecting plane normal is at the center of the projection. The angle δ measures the amount by which the rolling direction is rotated away from the left end of the axis AA' and has a value of +90° for the position illustrated. With these conventions the angles α and δ may be plotted on the pole figure in the same way as in the transmission method [Fig. 9-13(b)].

The great virtue of the Schulz method is that no absorption correction is required for values of α between 90° and about 40°, i.e., up to about 50° from the center of the pole figure. In other words, a random specimen can be rotated over this range of α values without any change in the measured intensity of the diffracted beam, provided the specimen has effectively infinite thickness. Under these circumstances, the intensity of the diffracted beam is directly proportional to the pole density in the specimen, without any correction. The constancy of the absorption factor is due essentially to the narrow horizontal slit placed in the primary beam at D (Fig. 9-16), close to the specimen. The vertical opening in this slit is only about 0.5 mm, which means that the specimen is irradiated only over a long narrow rectangle centered on the fixed axis AA'. It can be shown [9.13] that a change in absorption does occur, as the specimen is rotated about AA', but it is exactly canceled by a change in the volume of diffracting material, the net result being a

constant diffracted intensity for a random specimen when α lies between 90° and about 40°. To achieve this condition, the reflecting surface of the specimen must be adjusted to accurately coincide with the axis AA' for all values of α and δ. This adjustment is extremely important.

When the specimen is rotated out of the vertical position ($\alpha < 90°$) in the sense shown in Fig. 9-16, the top part moves behind, and the bottom in front of, the focusing circle. The diffracted beam therefore widens at the counter slit, and the measured diffracted intensity from a random specimen may decrease as α departs from 90°. This effect is called the *defocusing error*. It may be minimized by slit adjustment (widening the counter slit and decreasing the vertical opening in slit D) or corrected by calculation [9.14, 9.15].

Figure 9-17 shows a specimen holder suitable for either transmission method and for the Schulz reflection method.

The *Field and Merchant reflection method* [9.16] is designed for a parallel incident beam, shown simply as a single line in Fig. 9-18. The specimen is placed initially with the rolling direction vertical, coincident with the diffractometer axis, the transverse direction horizontal, and the plane of the sheet equally inclined to the

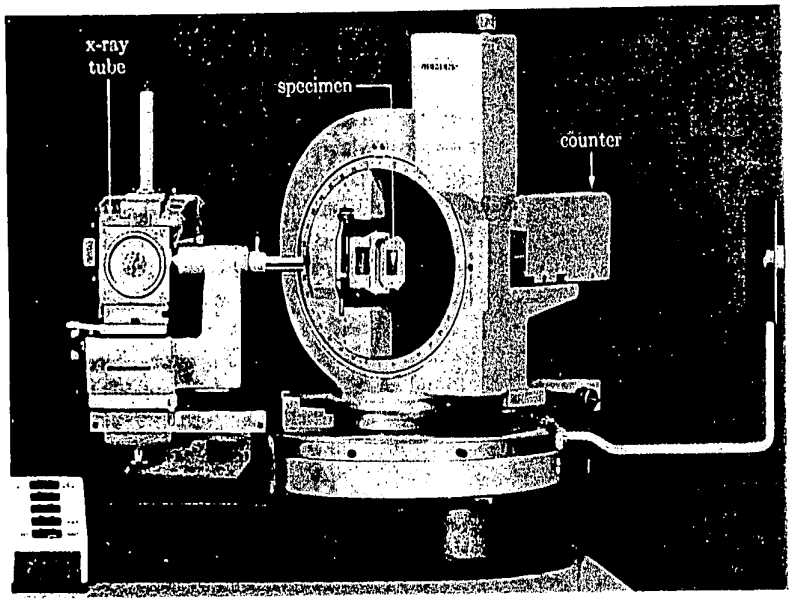

Fig. 9-17 Pole-figure goniometer. The specimen shown is positioned for measurements by the transmission method, and a simple change in the orientation of the specimen holder allows measurements by the Schulz reflection method. The x-ray tube is seen here end-on. This instrument is designed for automatic operation. (Courtesy of Siemens Corporation.)

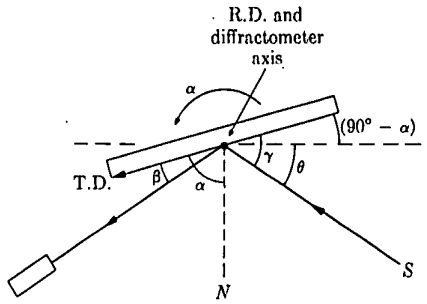

Fig. 9-18 Field and Merchant reflection method. N = diffracting plane normal.

incident and diffracted beams; the pole N of the reflecting plane is then at the center of the projection ($\alpha = 90°$). Counterclockwise rotation of the specimen about the diffractometer axis, which incidentally will narrow the diffracted beam, moves N to the left along the equator ($\delta = 0$) of the pole figure. The angle δ is changed by rotating the specimen in its own plane.

Reflected intensities must be corrected for change in absorption due to change in α. The angles γ and β of incidence and reflection are the same as shown in Fig. 4-19, and Eq. (4-14) applies:

$$dI_D = \frac{I_0 ab}{\sin \gamma} e^{-\mu x(1/\sin\gamma + 1/\sin\beta)}\, dx. \tag{4-14}$$

For counterclockwise rotation $\gamma = \theta + (90° - \alpha)$ and $\beta = \alpha - (90° - \theta)$. Making these substitutions into Eq. (4-14) and integrating from $x = 0$ to ∞, we find the integrated intensity:

$$I_D = \frac{I_0 ab}{\mu\{1 - [\cos(\alpha - \theta)/\cos(\alpha + \theta)]\}}. \tag{9-11}$$

We are interested only in the ratio of this quantity to the same quantity for $\alpha = 90°$. This ratio is

$$S = \frac{I_D(\alpha = \alpha)}{I_D(\alpha = 90°)} = 1 - \cot\alpha \cot\theta. \tag{9-12}$$

Diffracted intensities must be divided by S, which is independent of μ, to give values proportional to pole density. The correction is less severe (S closer to 1), the larger the value of θ; it is therefore advantageous to measure a higher order of the *hkl* reflection measured in transmission. The specimen holder can be identical with that used in the transmission method.

Plotting the Pole Figure

A transmission method yields pole densities covering the outer part of the pole figure, from $\alpha = 0$ to about 50°. A reflection method covers the inner part, from $\alpha =$ about 40° to 90°. The pole densities are in arbitrary units, either directly measured diffracted intensities or corrected intensities, depending on the method

used. Along those radii of the pole figure where substantial pole density exists in the region of overlap of the two methods (α = 40° to 50°), a normalizing factor is found which will make the pole densities from the transmission method agree with those from the reflection method. The match in the overlap region is rarely perfect, but a substantial disagreement between normalizing factors for different radii points to experimental or computational errors.

Once one set of data is normalized to match the other set, numbers proportional to pole density can be written on the pole figure at each point at which a measurement was made. Contour lines are then drawn at selected levels to connect points of the same pole density, and the result is a pole figure such as Fig. 9-19. Many, but not all, textures are symmetrical with respect to reflection planes normal to the rolling and transverse directions, and many published pole figures have been determined from measurements made only in one quadrant, with the other quadrants found by assuming symmetry, without supporting data.

The deformation texture of brass sheet (Fig. 9-19) is fairly sharp, and it is then of interest to know whether or not it can be approximated by an "ideal orientation." To find this orientation we successively lay several standard projections over the pole figure, looking for a match between (111) poles and high-density regions. The solid triangles in Fig. 9-19 show such a match; they represent the (111) poles of a single crystal oriented so that its (110) plane is parallel to the sheet and the $[\bar{1}12]$ direction parallel to the rolling direction. Reflection of these poles in the

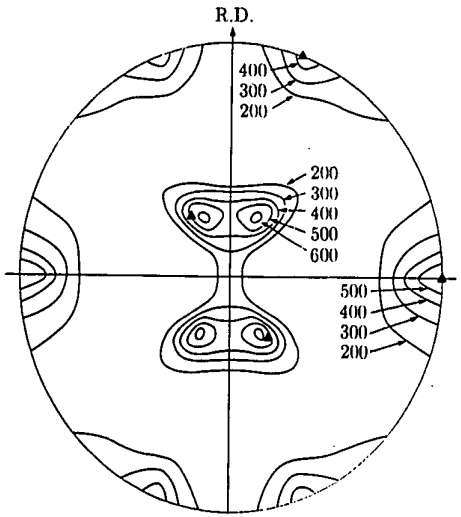

Fig. 9-19 (111) pole figure of alpha brass sheet (70 Cu–30 Zn), cold rolled to a reduction in thickness of 95 percent. Pole densities in arbitrary units. The outer parts of all four quadrants were determined experimentally; the inner parts of the upper right and lower left quadrants were measured, and the other two constructed by reflection. The solid triangles show the (110) $[\bar{1}12]$ orientation. Hu, Sperry, and Beck [9.17].

symmetry planes of the texture, which is equivalent to adding orientations like $(110)[1\bar{1}2]$, will approximately account for all the high-density regions of the pole figure. This texture can therefore be represented by the ideal orientation $\{110\}\langle\bar{1}12\rangle$. But the pole figure itself must be regarded as a far better description of the texture than any bare statement of an ideal orientation, which says nothing about the scatter. A quantitative pole figure has about the same relation to an ideal orientation as an accurate contour map of a hill has to a statement of the height, width, and length of the hill.

Pole densities in arbitrary units are not as informative as those expressed in multiples of the pole density of a random specimen, so called "times random" units. The contour lines in Fig. 9-20 are marked with these units, and one can see at a glance those regions of the pole figure that have a higher, or lower, pole density than random; this pole figure, incidentally, was measured in all four quadrants. The texture represented there, of considerable industrial interest, is messy and cannot be well characterized by ideal orientations. It is approximately a $\langle 111\rangle$ fiber texture, with the fiber axis normal to the plane of the sheet, containing $\{111\}\langle 110\rangle$, called the "cube-on-corner" texture, as its strongest single component [9.18, 9.19].

Diffracted intensities, proportional to pole densities, may be put on a times-random basis by comparing them with intensities diffracted by a random specimen [9.20]. The random specimen should be of the same material as the textured specimen and, for a transmission method, it should have the same value of μt; if not, a correction has to be made that will depend on the transmission method involved. The random specimen itself is usually made by compressing and sintering a powder [9.11, 9.12]. The randomness of grain orientation in this specimen must be checked by determining its diffraction pattern with a diffractometer in the usual way; the measured integrated intensities of all lines should agree with those calculated by Eq. (4-21).

General

The conditions for optimum specimen thickness in transmission and infinite thickness in reflection are such that the same specimen can serve for both methods. The penalty for exceeding the optimum thickness is not severe: a thickness of double the optimum value for transmission at $\alpha = 0$ reduces the diffracted intensity by only 26 percent (Problem 9-8).

It may be difficult to make a thin specimen, particularly of a heavy metal, which has the required low, and *uniform*, value of μt throughout. Some investigators have therefore avoided a transmission method altogether by determining only the central portion of the pole figure by reflection; such partial pole figures are useful for some purposes. Others have obtained a complete pole figure by reflecting x-rays from a surface or surfaces inclined to the sheet surface. Several pieces of the sheet are stacked with rolling directions parallel and a composite specimen made by clamping or cementing the stack. If this specimen is cut to expose a surface whose normal makes the same angle, of 54.7°, with the sheet normal and rolling and transverse directions, then measurements on this surface

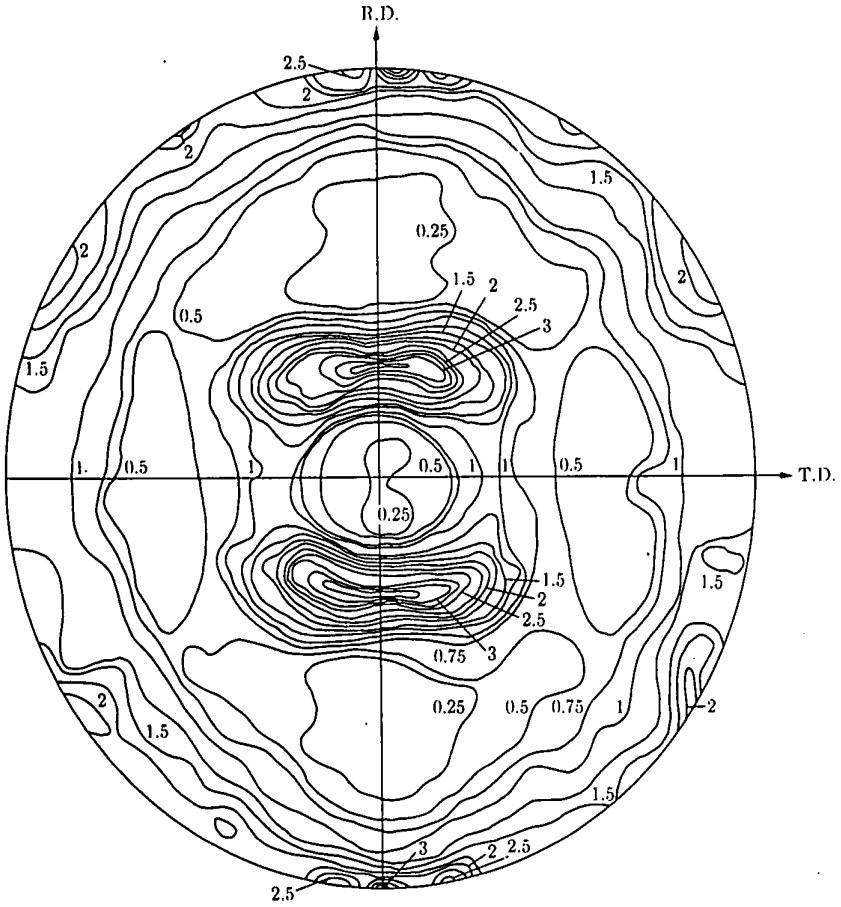

Fig. 9-20 (110) pole figure of recrystallized commercial low-carbon (0.04 percent) sheet steel, aluminum killed, 0.9 mm thick. Pole densities in "times random" units. Determined by a reflection method from composite specimens; see text under "General." Bunge and Roberts [9.18].

by a reflection method will cover one quadrant of the pole figure [9.21]. The pole figure of Fig. 9-20 was derived from reflection measurements on the sheet plane and on sections normal to the rolling and transverse directions.

Some errors that can affect texture measurements are the following:

1. If the grain size is too large, as in some recrystallized specimens, the incident beam will not sample enough grains for good statistical accuracy. The specimen holder should then include a mechanical device that will translate the specimen back and forth in its own plane in order to expose more grains to the incident beam.

2. The texture at the surface of a sheet can differ from that in the midplane [9.17].

When such a texture gradient exists, it must be remembered that the transmission and reflection methods preferentially sample different layers of the same specimen and that the thicknesses of the layers so sampled vary with α in a systematic way.

3. The x-ray optics, particularly slit sizes, must conform to those required by the x-ray method involved. Too narrow a counter slit will exclude a wanted part of the diffraction line; too wide a slit will include some of the background. Too often the background is simply ignored, with the result that measured intensities include both line and background; it would be highly beneficial to eliminate or reduce the background by means of a crystal monochromator, balanced filters, or a pulse-height analyzer. Errors from these sources can be large. They can be almost entirely eliminated by comparing intensities from the textured specimen with intensities measured under identical conditions from a truly random specimen, provided the two specimens differ *only* in grain orientation. Such a random specimen can be very hard to make. (Note, for example, that an annealed random specimen will have narrower diffraction lines than a cold-worked textured specimen.)

Because the manual determination of preferred orientation is rather tedious, the process has been automated by laboratories that need large amounts of this kind of data [9.22-9.27]. Under computer control, the angular settings α and δ of the specimen are varied in a prescribed sequence by motor drive, and the diffracted intensity at each setting is recorded, on paper tape, for example. These output data can also be used to control an automatic pole-figure plotter. Apparatus of this kind is commercially available, such as that shown in Fig. 9-17.

The *analysis* of preferred orientation has now gone beyond pole figures, in the direction of a more complete description of the texture. When we establish experimentally that a certain crystal in a sheet has a (100) pole, for example, located at a point on the pole figure specified by the angles α and δ, we have not fully specified the orientation of the crystal. These two angles merely describe the orientation of the direction [100], and the crystal might have any rotational position about this axis. A third angle is needed to fix the orientation of the crystal. A full description of the texture would require the specification of three angles (called ψ, θ, ϕ) for each crystal in the sheet. This information is contained in the *crystal orientation distribution*, and methods of calculating this distribution from pole figures have been developed by Roe, Bunge, and Williams [9.29-9.32]. The mathematics involved are complex and the calculations extensive, but this approach is powerful and of great generality.

The crystal orientation distribution for a cubic material in sheet form can be calculated from any two experimental pole figures, for example, the (100) and (110). Once the distribution is known, any other desired pole figure can be calculated, for example, the (111); it need not be measured. It is even possible to calculate the orientation distribution from a set of partial pole figures, determined by a reflection method out to 60° from the center of the pole figure ($\alpha = 30°$) [9.28]. The crystal orientation distribution itself is usually presented in the form of crystal density plots, in which the density is shown as a contour map on, for example, ψ, θ axes with ϕ held constant; a series of such constant-ϕ maps is needed to

present all the information. Applications of the orientation distribution approach may be found in [9.18, 9.19, 9.28, 9.33, 9.34].

Finally, we must not forget that the practical reason for investigating preferred orientation is to understand the properties of the aggregate. The old problem still remains: how do we calculate the physical and mechanical properties of an aggregate from the corresponding properties of the single crystal and the measured texture? The crystal orientation distribution affords the most rational basis so far available for this calculation, and considerable progress has been made in this direction [9.18, for example].

9-9 THE TEXTURE OF WIRE (DIFFRACTOMETER METHOD)

As mentioned in Sec. 9-6, if a wire or rod has a true fiber texture, its pole figure will have rotational symmetry about the fiber axis and will resemble Fig. 9-8. We therefore have to measure pole density only along a single radius. The angle between the pole N and the fiber axis F.A. is usually called ϕ, rather than α, when dealing with fiber textures.

The Field and Merchant method may be used to measure pole density, and two specimens are required to cover the entire 90° range of ϕ:

1) *Low-ϕ region.* X-rays are reflected from the cross section of the wire, as in Fig. 9-21(a). The specimen is a bundle of wires, packed together and cemented into a rectangular hole cut in a thick plastic disc; the wire ends are then ground, polished, and etched. This cross section is made initially parallel to the diffractometer axis and equally inclined to the incident and diffracted beams. The angle ϕ measures the counterclockwise rotation of the specimen about the diffractometer axis from this initial position, and we define a new angle ρ as the acute angle between the specimen surface and the reflecting-plane normal N. The angle α of Eq. (9-12) and Fig. 9-18 becomes $\rho = \rho_L = 90° - \phi$, so that

$$W = \frac{I_D(\rho = \rho)}{I_D(\rho = 90°)} = 1 - \cot \rho \cot \theta. \qquad (9\text{-}13)$$

Diffracted intensities are to be divided by W to obtain numbers proportional to pole density.

2) *High-ϕ region.* X-rays are reflected from the side of the wire, as in Fig. 9-21(b). The specimen is a set of wires glued to a grooved plate. Equation (9-13) still applies, but now $\alpha = \rho = \rho_H = \phi$.

When the diffracted intensities I_D given by each method have been divided by W and normalized in the region of overlap, we have a set of numbers I proportional to pole density. Figure 9-22 shows an I, ϕ curve obtained in this way for the inside texture of cold-drawn aluminum wire. The peaks at $\phi = 0$ and 70° are due to the strong [111] component of the texture and the peak at 55° to a weak [100] component.

By analysis of an I, ϕ pole density curve we can (a) put pole densities on a times-random basis and (b) determine the relative amounts of the components in a double fiber texture [9.36–9.38].

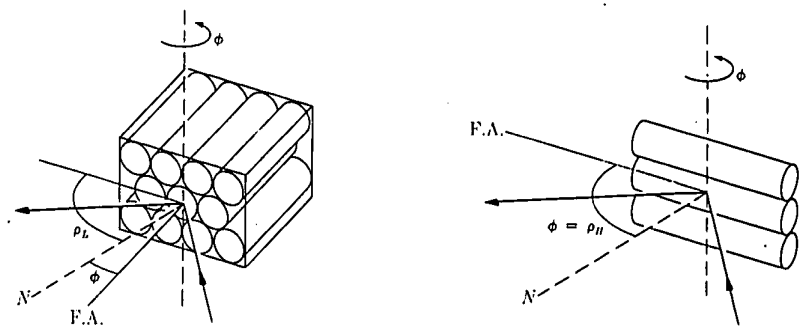

(a) Low-ϕ region (b) High-ϕ region

Fig. 9-21 Reflection from composite wire specimens. ϕ is angle between fiber axis F.A. and reflecting-plane normal N. ρ is angle between N and specimen surface.

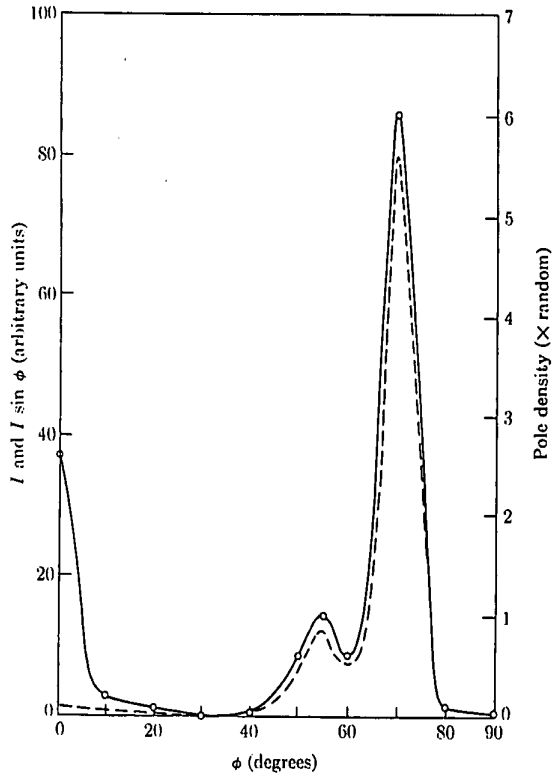

Fig. 9-22 (111) pole density I (full curve) and I sin ϕ (dashed) as a function of ϕ for a cold-drawn aluminum wire, reduced in area 95 percent by drawing, and etched to 80 percent of the as-drawn diameter. Final specimen diameter 1.3 mm, Cr $K\alpha$ radiation, 222 reflection. Freda *et al.* [9.35].